Magn Reson Mater Phy (2007) 20:169–173
DOI 10.1007/s10334-007-0079-x

SHORT COMMUNICATION

In vivo mouse spinal cord imaging using echo-planar imaging at 11.75 T

Virginie Callot · Guillaume Duhamel · Patrick J. Cozzone

Received: 13 April 2007 / Revised: 31 May 2007 / Accepted: 29 June 2007 / Published online: 28 July 2007

Abstract
Object To evaluate the feasibility of mouse spinal cord MR imaging using echo-planar imaging (EPI).
Materials and methods Optimized multi-shot spin-echo-EPI sequences were compared to conventional spin-echo (c-SE) at 11.75 T and used for high-spatially resolved acquisitions and relaxation-time measurements.
Results Good quality images were obtained, with clear delineation of gray and white matter. Acquisition-time gain factor was up to 6 (vs. c-SE) and resolution up to $74 \times 94\ \mu m^2$ was achieved. T_1 and T_2 relaxation times were reliably measured.
Conclusion High-temporally and spatially resolved mouse spinal cord EPI imaging is feasible. This technique should greatly benefit to long acquisition-time experiments (diffusion imaging) and imaging of rapidly-evolving pathologies.

Keywords MRI · Echo planar imaging (EPI) · Spinal cord · Mouse · High-field

Introduction

Nowadays, mouse models are commonly employed to study spinal cord (SC) pathologies, such as multiple sclerosis or trauma, or to test new therapeutic and regenerative strategies.

To allow a longitudinal follow-up and assessment of physiopathological mechanisms and drug efficacy, non-invasive imaging techniques, such as magnetic resonance imaging (MRI), are required and henceforth frequently used [1–4]. However, performing mouse SC MRI remains a challenging undertaking, mainly due to the small size of the spine. To achieve adequate resolution and signal-to-noise ratio (SNR), high-field MRI appears appropriate and most of the reported mice studies have consequently been performed at 4.7 [2] or 9.4 T [1,5–7]. On the other hand, the acquisition of spatially resolved SC images is time-consuming, especially when functional imaging, such as diffusion imaging, is also performed. In these cases, as well as in cases of rapidly evolving pathology, rapid imaging techniques would be valuable.

Echo-planar imaging (EPI), which is one of the fastest MR techniques, is largely applied for human SC imaging; it has also been used for rat studies at 2 [8] and 7 T [9,10], but, to our knowledge, it has never been applied for mouse SC investigation. Ghosting and susceptibility-induced artifacts of EPI sequences on high-field MR systems may explain why EPI has not been extensively used for rodent studies. Recent improvements in the technology (gradient system, pre-emphasis correction...) have, however, led to a distinct increase of EPI image quality.

In this study, we have investigated whether high-field MRI (11.75 T) on mouse spinal cord using EPI was feasible and capable to provide images of high-temporal and spatial resolution.

Materials and methods

Experimental setup

All experiments were performed on an 11.75 T vertical Bruker Avance 500 MHz/89 mm wide bore vertical imager

V. Callot and G. Duhamel equally contributed to this work.

V. Callot (✉) · G. Duhamel · P. J. Cozzone
Centre de Résonance Magnétique Biologique et Médicale (CRMBM), UMR CNRS n°6612, Faculté de Médecine de Marseille, Université de la Méditerranée, 27 Bd Jean Moulin, 13385 Marseille Cedex 5, France
e-mail: virginie.callot@medecine.univ-mrs.fr

(Bruker, Ettlingen, Germany), with high-performance actively shielded gradients (1 T/m maximum gradient strength, 9 kT/m/s maximum slew rate), and integrated second-order shim.

Healthy mice (C57BL/6, $n = 3$, age 14/15 weeks, body weight 25/30 g) were anesthetized by spontaneous respiration of a mixture of air and 1.7% isoflurane (flow rate 267 ml/min, Univentor 400 anesthesia unit (Univentor, Zejtun, Malta)), to obtain regular breathing at a frequency of 85–90 breaths per minute. The animals were positioned head up on an animal bed in a 3-cm diameter transmitting/receiving birdcage coil (homogenous length 5 cm, Micro2.5Probe, Bruker, Ettlingen, Germany). Respiration was monitored throughout the experiment using a pressure sensor placed under the abdomen of the mouse (SA instruments Inc., NY, USA).

EPI adjustments

A spin-echo EPI (SE-EPI) sequence was used for all acquisitions. Several manufacturer features, such as automatic shimming, pre-emphasis correction, B_0 shift compensation, and automatic ghost correction, ensured a limitation of ghost and distortion artifacts.

The sampling bandwidth (BW) was set to 400 kHz as a compromise between reduction of distortions and loss of SNR. Multi-shot EPI acquisitions (2, 4, 8-shots) were investigated in order to increase the effective bandwidth; the readout module was shifted in the sampling window (echo shift 18%) to further reduce the echo-time. The signal was sampled continuously throughout the echo train and during the gradient ramps. Regridding reconstruction was performed by the manufacturer algorithm. Off-resonance artifacts were eliminated by using a fat suppression module.

MR parameters

Seven axial reference scans, identified from a sagittal image and covering the cervical segments C1–C7, were acquired using a gradient-echo (GE) sequence (TE/TR 1.74/30 ms, RF flip angle 15°, FOV 17 × 17 mm^2, slice thickness 0.75 mm, acquisition matrix 128 × 128 and number of experiments (NEX) 10). Axial images of identical spatial resolution were acquired using a conventional spin-echo (c-SE) (TE 10.67 ms, BW 50 kHz, NEX 1) and multi-shot SE-EPI sequences ($n = 1$, 2, 4 and 8-interleaved shots, TE = 23.06, 14.90, 10.67 and 8.60 ms, respectively, acquisition matrix 148 × 128 regridded to 128 × 128 and NEX 5). The NEX value was empirically determined to provide similar SNR between the c-SE and the 4-shot SE-EPI sequences. Both c-SE and SE-EPI sequences were synchronized with the animal breathing (85 breaths/min), leading to a repetition time for the seven slice acquisition of approximately 5 s.

To illustrate the feasibility of functional imaging with EPI, T_1 and T_2 measurements were then performed using the 4-shot SE-EPI sequence. Seven T_1-weighted images (C1–C7) were acquired using an inversion-recovery technique (TR/TE 10,000/10.67 ms, NEX 9, 4 ms adiabatic hyperbolic secant inversion pulse) with seven inversion times (TI = 0.13, 0.53, 0.9, 1.4, 1.7, 4 and 9 s). T_2 measurements were obtained from separated T_2-weighted images acquired at different TE (TE = 20, 30, 50, 60 and 70 ms, TR 10 s and NEX 5) at the C1–C7 levels.

Finally, high-spatially resolved images were acquired, with the 4-shot EPI sequence, using the following parameters: FOV 9.5 × 15 mm^2, acquisition matrix 148 × 160 regridded to 128 × 160, TE 14 ms and NEX 10).

Data processing

Data processing was performed using in-house-developed softwares running under IDL (Research Systems Inc., Boulder, USA). T_1 and T_2 maps were generated by fitting pixel-by-pixel the standard inversion recovery function ($S(\mathrm{TI}) = S_0 \,.\, (1 - 2 \,.\, \exp(-\mathrm{TI}/\mathrm{T}_1))$ and the spin-echo attenuation function ($S(\mathrm{TE}) = S_0 \,.\, \exp(-\mathrm{TE}/\mathrm{T}_2)$) to the signal intensity S of the T_1-weighted and T_2-weighted images series, respectively, (with S_0 a constant proportional to the spin density).

Regions of interest (ROI) were manually selected in the white (WM) and gray (GM) matter. Mean T_1 and T_2 values were calculated for each of the seven slices and each animal and then averaged.

Student's t-tests were carried out for comparison between GM and WM values (JMP software, SAS Inc., Cary, USA).

Results

Anatomical images

In vivo axial images (133 × 133 μm^2 in-plane resolution) acquired at different cervical levels with the multi-shot SE-EPI, the c-SE and GE sequences are shown on Fig. 1.

Distortions of SE-EPI images are greatly reduced by increasing the number of EPI-shots. The 4- and 8-shot images present aspects similar to those acquired with c-SE and GE and the gross morphology of the cord, including white and gray matter and dorsal and ventral horns, can be easily distinguished. Similar SNR values were obtained for both 4-shot SE-EPI and c-SE acquisitions. Due to increased susceptibility-induced gradients in the tissues at the lower level (C6–C7), image distortions are more pronounced and the spinal cord appears with a shrunk aspect (varying between 0.25 and 1.5 pixels), even with the 8-shot sequence.

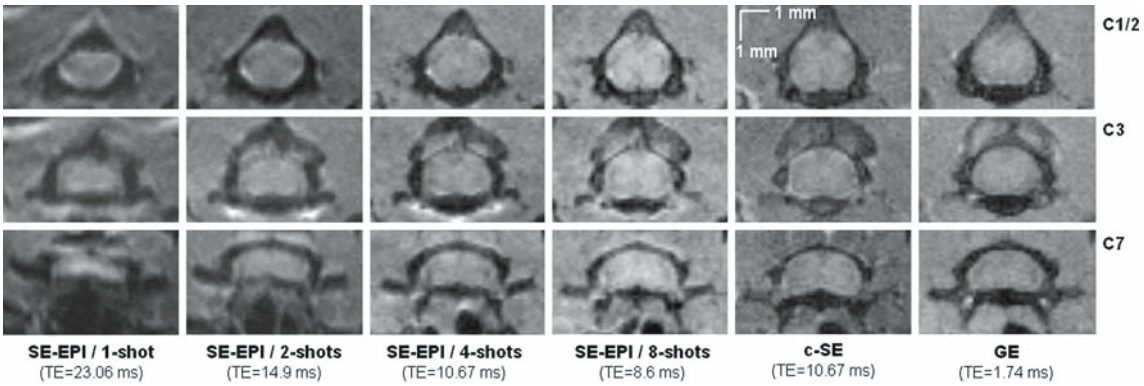

Fig. 1 From left to right: 1-, 2-, 4- and 8-shot spin-echo EPI (SE-EPI), conventional spin-echo (c-SE) and gradient-echo (GE) images, acquired at the level of C1/C2, C3 and C7. In-plane resolution is identical for each sequence (133 × 133 μm^2). Scan times for the acquisition of the seven slice series (C1–C7) are, respectively, equal to: 0.42, 0.83, 1.66, 3.33, 10.67 and 4.48 min

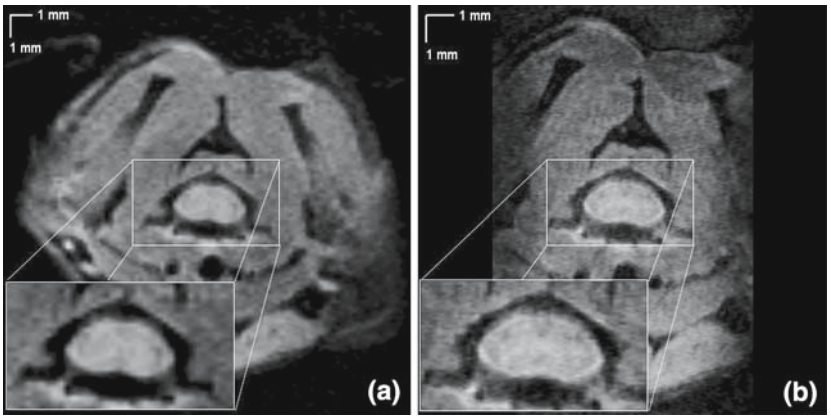

Fig. 2 4-Shot SE-EPI images (TE 14 ms, NEX 10, slice thickness 0.75 mm, total acquisition time 3.33 min). Resolutions (voxel volumes) are: **a** 133 × 133 μm^2 (13.3 nl) and **b** 74 × 94 μm^2 (5.2 nl)

Figure 2b depicts a high-spatially resolved image (74 × 94 μm^2), for which border delineation of the structures (white matter, spinal roots) is clearly improved compared to the 133 × 133 μm^2 resolution image (Fig. 2a). Both images were acquired with 10 NEX; this accounts for the observed difference in SNR.

In vivo relaxation times

Example of T_2-weighted images and resultant T_2 map are shown in Fig. 3a. Gray matter appears slightly hypointense compared to white matter. The mean T_2 values ($n = 3$ mice) have been found equal to 27.49 ± 1.39 ms for GM and 39.60 ± 0.77 for WM ($P = 0.0002$).

Example of T_1-weighted images and resultant T_1 map are shown on Fig. 3b. The contrast between GM and WM matter is very low, indicating that both WM and GM have similar longitudinal relaxation time. This was confirmed by the measured mean T_1 values ($n = 3$ mice): 1.87 ± 0.10 s for GM and 1.82 ± 0.14 for WM ($P = 0.379$).

Discussion

The purpose of this work was to investigate whether the use of EPI would provide satisfactory images of mouse spinal cord and thus be valuable for fast functional imaging of the spine.

The 4- and 8-shot SE-EPI techniques described in this work allows the visualization of internal structures such as gray and white matter, and give images of good quality, with few distortions.

Seven-slice series, covering the entire cervical spine, have been acquired in less than 2 min with the 4-shot EPI sequence (3.3 min with the 8-shots), against 10.7 min for the conventional c-SE sequence; i.e., by using EPI technique rather than conventional techniques, the acquisition time can be decreased by a factor up to six for routine spatial resolution of 133 × 133 μm^2, without loss of SNR. The highest resolution achieved in this study was 74 × 94 μm^2. These resolutions are similar to those obtained with conventional imaging, as found in literature (from 125 to 200 μm^2 [1,4,5] for routine resolution and 60 to 80 μm^2 [2,5,7] for high resolution).

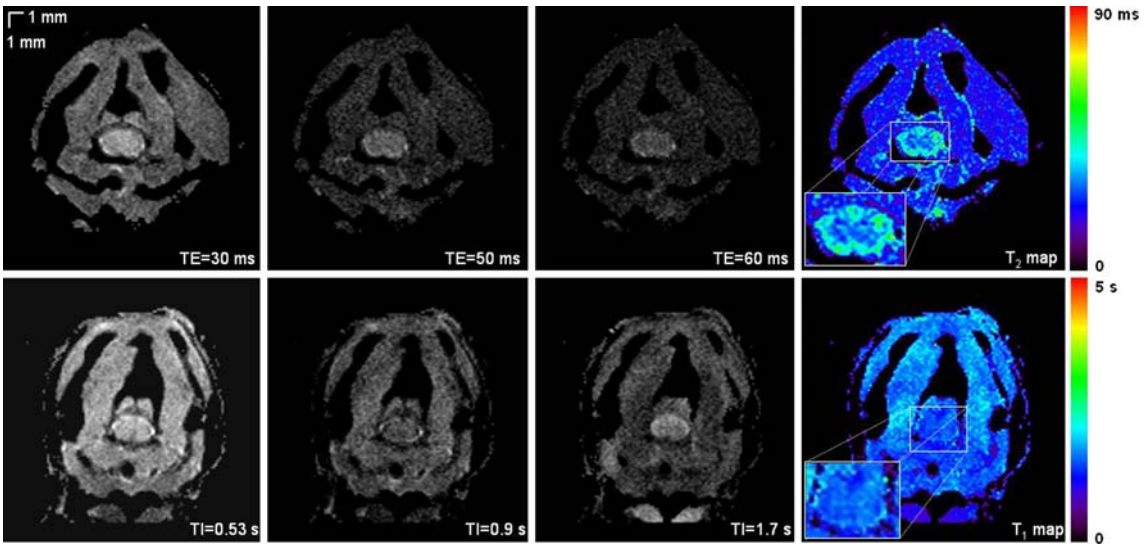

Fig. 3 From left to right: **a** T_2-weighted images for different TE and the resultant T_2 map; **b** T_1-weighted images for different TI and the resultant T_1 map

The longitudinal and transversal relaxation times were measured in the gray and white matter under full-relaxation conditions. The GM/WM averaged values we obtained (respectively (1.87 ± 0.10) s and (1.82 ± 0.14) s for the T_1 and (27.49 ± 1.39) ms and (39.60 ± 0.77) ms for the T_2) are in concordance with those obtained by other groups with conventional SE sequences at lower fields. At 9.4 T, Bilgen et al. [5] measured T_1 values of 1.73 and 1.69 s and T_2 values of 32.6 and 38.1 ms for GM/WM, respectively (with TR = 4 s); at 7 T, on rats, Franconi et al. [11] measured T_2 values of 43.2 and 57 ms (with TR = 2.5 s).

To our knowledge, this study is the first that uses EPI technique for mouse SC investigation. Moreover, it is the first report of mouse SC MRI at very high field ($B_0 > 9.4$ T) since previous reports pertained to rats [12].

Drawbacks of the method mainly include distortions caused by the bony structure and by field-inhomogeneity. Our experiments focused on imaging in the axial plane, which provides the best orientation for distinguishing WM from GM and only residual and acceptable distortions. However, EPI would be precluded for imaging along the longitudinal axis, due to higher field-inhomogeneities.

Then, decomposing the experiments into several shots may have deprived EPI from its immunity to signal variations as compared to single-shot EPI. However, respiratory gating and constant breathing rate have ensured stability.

Finally, although much care must be taken in EPI pre-adjustments (echo-time optimization, pre-emphasis calibration, ghost correction . . .), the results presented in this work show that, with high-quality gradients and shim systems, obtaining good image quality with EPI at high field is feasible. Moreover, time necessary for EPI adjustments does not exceed 5 min.

The method may, therefore, be very valuable when series or multiple sets of images from the SC are needed. For instance, diffusion tensor imaging, which usually requires long acquisition time, and imaging of rapidly evolving conditions such as contusion and second injury, may greatly benefit from the technique. EPI may also be used to decrease the anesthesia time (and potential associated mortality) or to monitor therapeutic intervention.

Conclusion

In this work, we demonstrated that high-temporally and spatially resolved mouse spinal cord EPI imaging, at high-field, is feasible.

References

1. Bonny JM, Gaviria M, Donnat JP, Jean B, Privat A, Renou JP (2004) Nuclear magnetic resonance microimaging of mouse spinal cord in vivo. Neurobiol Dis 15:474–482
2. Kim JH, Budde MD, Liang HF, Klein RS, Russell JH, Cross AH, Song SK (2006) Detecting axon damage in spinal cord from a mouse model of multiple sclerosis. Neurobiol Dis 21:626–632
3. Pirko I, Ciric B, Gamez J, Bieber AJ, Warrington AE, Johnson AJ, Hanson DP, Pease LR, Macura SI, Rodriguez M (2004) A human antibody that promotes remyelination enters the CNS and decreases lesion load as detected by T2-weighted spinal cord MRI in a virus-induced murine model of MS. Faseb J 18:1577–1579
4. Stieltjes B, Klussmann S, Bock M, Umathum R, Mangalathu J, Letellier E, Rittgen W, Edler L, Krammer PH, Kauczor HU, Martin-Villalba A, Essig M (2006) Manganese-enhanced magnetic resonance imaging for in vivo assessment of damage and functional improvement following spinal cord injury in mice. Magn Reson Med 55:1124–1131

5. Bilgen M, Al-Hafez B, Berman NE, Festoff BW (2005) Magnetic resonance imaging of mouse spinal cord. Magn Reson Med 54:1226–1231
6. Gaviria M, Bonny JM, Haton H, Jean B, Teigell M, Renou JP, Privat A (2006) Time course of acute phase in mouse spinal cord injury monitored by ex vivo quantitative MRI. Neurobiol Dis 22:694–701
7. Bilgen M (2004) Simple, low-cost multipurpose RF coil for MR microscopy at 9.4 T. Magn Reson Med 52:937–940
8. Fenyes DA, Narayana PA (1999) In vivo diffusion characteristics of rat spinal cord. Magn Reson Imaging 17:717–722
9. Deo AA, Grill RJ, Hasan KM, Narayana PA (2006) In vivo serial diffusion tensor imaging of experimental spinal cord injury. J Neurosci Res 83:801–810
10. Madi S, Hasan KM, Narayana PA (2005) Diffusion tensor imaging of in vivo and excised rat spinal cord at 7 T with an icosahedral encoding scheme. Magn Reson Med 53:118–125
11. Franconi F, Lemaire L, Marescaux L, Jallet P, Le Jeune JJ (2000) In vivo quantitative microimaging of rat spinal cord at 7 T. Magn Reson Med 44:893–898
12. Behr VC, Weber T, Neuberger T, Vroemen M, Weidner N, Bogdahn U, Haase A, Jakob PM, Faber C (2004) High-resolution MR imaging of the rat spinal cord in vivo in a wide-bore magnet at 17.6 Tesla. Magma Magn Reson Mater Phy 17:353–358